Geotechnical Engineering
Volume 168 Issue GE5

Behaviour of concrete-face rockfill dam on sand and gravel foundation
Wen, Chai, Wang *et al.*

ice | proceedings

Proceedings of the Institution of Civil Engineers
Geotechnical Engineering 168 October 2015 Issue GE5
Pages 439–456 http://dx.doi.org/10.1680/geng.14.00103
Paper 1400103
Received 03/06/2014 Accepted 19/12/2014
Published online 27/02/2015
Keywords: dams, barrages & reservoirs/field testing & monitoring/foundations
ICE Publishing: All rights reserved

ice Institution of Civil Engineers publishing

Behaviour of concrete-face rockfill dam on sand and gravel foundation

1 **Lifeng Wen** MEng
PhD student, State Key Laboratory Base of Eco-hydraulic in Arid Area, Xi'an University of Technology, Xi'an, People's Republic of China

2 **Junrui Chai** PhD
Professor of Civil and Geotechnical Engineering, State Key Laboratory Base of Eco-hydraulic in Arid Area, Xi'an University of Technology, Xi'an, People's Republic of China; also College of Hydraulic and Environmental Engineering, China Three Gorges University, Yichang, People's Republic of China

3 **Xiao Wang** MEng
Geotechnical Engineer, State Key Laboratory Base of Eco-hydraulic in Arid Area, Xi'an University of Technology, Xi'an, People's Republic of China

4 **Zengguang Xu** PhD
Associate Professor, State Key Laboratory Base of Eco-hydraulic in Arid Area, Xi'an University of Technology, Xi'an, People's Republic of China

5 **Yuan Qin** PhD
Lecturer, State Key Laboratory Base of Eco-hydraulic in Arid Area, Xi'an University of Technology, Xi'an, People's Republic of China

6 **Yanlong Li** PhD
Associate Professor State Key Laboratory Base of Eco-hydraulic in Arid Area, Xi'an University of Technology, Xi'an, China



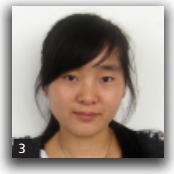


An increasing number of dams are being built on deep sand and gravel foundations. In this paper, the stress–deformation behaviour of a concrete-face rockfill dam built on sand and gravel foundation is studied based on in situ monitoring results and finite-element analysis. The effects of a dam construction scheme on the behaviour of the dam and its impervious structures are discussed. The stress and deformation values that were computed using the finite-element analysis model are consistent with the measured data. The monitored data and numerical results indicate that maximum settlement occurred at the bottom of the dam and maximum compressive stress is distributed in the foundation. The concrete-face rockfill dam built on the sand and gravel foundation exhibited good performance. The staged construction scheme of the dam caused uneven deformation and stress concentration in the dam body but could improve the behaviour of the cut-off wall to a certain extent. Moreover, several factors that influence the behaviour of the cut-off wall are analysed.

1. Introduction

Given their advantages of adaptability to topography and geology, increasing numbers of concrete-face rockfill dams (CFRDs) have been and are being built on poor foundations. Deep sand and gravel foundation is a typically complex geological condition characterised by looseness, lithology discontinuance, complex genetic type and greater unevenness in its physical and mechanical structure (Gikas and Sakellariou, 2008; Ito and Azam, 2013; Szostak *et al.*, 2005; Wang and Liu, 2005). Given the massive amount of sand and gravel, a considerable number of CFRDs are being constructed with the toe slab, which is built directly on sand and gravel. Such an approach is expected to reduce investment and shorten the construction period. In these CFRDs, the concrete slab for the dam body and the cut-off wall for the foundation play an important role as impervious structures. Any cracks in these structures would affect the integrity of the seepage control system (Rice and Duncan, 2010a, 2010b). Deformation of impervious structures depends on the extent to which the rockfill

Downloaded by [UNIV OF ILLINOIS] on [05/02/20]. Copyright © ICE Publishing, all rights reserved.

and sand and gravel undergo distortion (Brown and Bruggemann, 2002; Karim *et al.*, 2010; Kim and Kim, 2008). To reduce the possibility of such risks in the CFRDs, understanding the behaviour of the dam and its impervious structures is essential. Such comprehensive understanding is expected to improve the design and construction of CFRDs built on sand and gravel foundations.

A number of case studies have investigated the behaviour of embankments built on soft foundations (Chai *et al.*, 2013; Dounias *et al.*, 2012; Haan and Feddema, 2012; Müller *et al.*, 2012; Özer and Bromwell, 2012). The mechanical properties of impervious structures have also attracted considerable research attention (Conti *et al.*, 2012; Hinchberger *et al.*, 2010; Li *et al.*, 2008; Segura and Aguado, 2012). Although significant achievements relating to the behaviour of CFRDs built on bedrock and the dynamic response of CFRDs built on sand and gravel layers have been reported (Feng *et al.*, 2010; Su *et al.*, 2012; Won and Kim, 2008), understanding of the behaviour of the dam and related impervious structures of CFRDs built on sand and gravel foundations remains limited.

This paper investigates the behaviour of a CFRD built on a sand and gravel foundation during the course of dam construction and reservoir filling, by monitoring the results and through numerical predictions. The effect of the dam construction scheme on the behaviour of the CFRD and its impervious structures is discussed. In addition, the effects of construction sequence and penetration depth of the cut-off wall on the behaviour of the wall are discussed.

2. Main features of the Miaojiaba CFRD

2.1 Miaojiaba CFRD

The Miaojiaba CFRD was built on Bailongjiang River in Wenxian City, Gansu Province, China (Figure 1), located 18·0 km upstream from the Guantou dam and 31·5 km downstream from the Bikou hydropower station. Figure 1(b) shows the maximum cross-section of the Miaojiaba CFRD. The dam is 111 m high, has a crest that is 348·20 m long and is 10·0 m wide. The dam has three generators in the downstream power station, which account for a total electricity generation capacity of 240 MW. The main parameters of the Miaojiaba project are shown in Table 1.

2.2 Site condition and seepage control system

The dam is located in an alpine gorge region. The site has deep river gravels with thickness that ranges from 44 m to 50 m. The river gravels from the bottom to the top are summarised as follows

(*a*) Q_4^{a1} – sand and gravel with block gravel layers, 5 m to 10 m thick
(*b*) Q_4^{a2} – sand and gravel (the major components of the foundation), 12 m to 15 m thick
(*c*) Q_4^{a3} – cobble (particles larger than gravel size), sand and gravel with gravel layers, 6 m to 20 m thick
(*d*) reservoir alluvium, 2 m to 4 m thick.

The river gravels mainly comprise sand and gravel. The mechanical properties of the sand and gravel have been analysed through field compaction tests and triaxial tests. Figure 2 shows the gradation curve of the sand and gravel. The gradation is continuous with a maximum particle size of 600 mm. The sand and gravel was compacted by a 25 t towed vibratory roller before the dam construction. A slot-type concrete cut-off wall with a depth of 50 m and thickness of 1·2 m was designed to control foundation seepage, as shown in Figure 1(b). The dam seepage control system is composed of cut-off wall, toe slab, connecting plate and face slab. The thickness of the upstream reinforced concrete face slab is 0·3 m at the top elevation of 805 m and 0·618 m at the bottom elevation of 700 m, with a linear varying relationship.

2.3 Construction materials and staged construction scheme

The total rockfill volume of the dam body is 3·77 million m^3. The mineral contents of the rockfill and transition materials are both thick, massive, metamorphic tuff, with compressive strength of 150 MPa. The cushion material is composed of artificial blended sand and gravel. The construction materials have different particle size distributions, as shown in Figure 2. The main rockfill and sub-rockfill materials are from the same quarry and have the same particle size distribution, but have different densities. The main rockfill has a density of 2·30 g/cm^3 and the sub-rockfill has a density of 2·15 g/cm^3. The details of the construction materials and methods are given in Table 2.

A staged construction scheme was used to construct the dam, as shown in Figure 3. Construction of the cut-off wall began in September 2009, 3 months earlier than the construction of the dam body, and was completed in October 2009. The entire section of the dam body was constructed to the elevation of 740 m in March 2010. Afterwards, from April to October 2010, the upstream and downstream sections were constructed to the elevation of 780 m, respectively. The downstream slope of the upstream section is 1:1·3. The construction of the dam body was completed in December 2010. The face slabs were constructed in January and February 2011. The power station started generating electricity by the end of July 2011.

3. Stress–deformation monitoring system

The behaviour of the Miaojiaba CFRD during the entire construction stage was observed using a comprehensive monitoring system that monitors the behaviour of the dam body and the cut-off wall. The vertical displacements inside the dam body were measured using electromagnetic settlement gauges and hydraulic overflow settlement gauges. The electromagnetic settlement gauges were distributed in the maximum cross-section of 0 + 192, with 45 monitoring points along three vertical monitoring lines, as shown in Figure 4(a). The hydraulic overflow settlement gauges were distributed in four critical cross-sections, namely,

Downloaded by [UNIV OF ILLINOIS] on [05/02/20]. Copyright © ICE Publishing, all rights reserved.

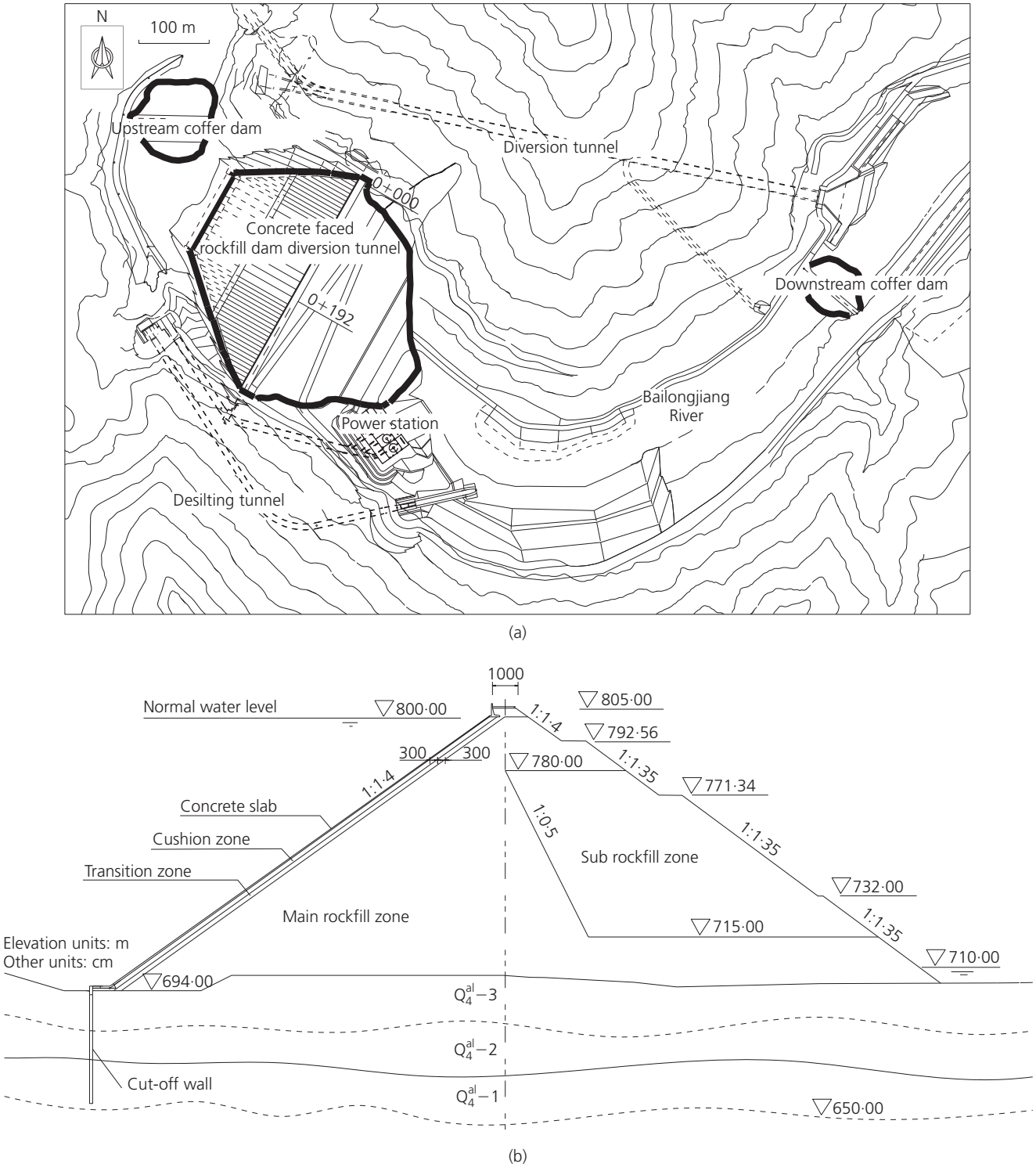

Figure 1. (a) Layout of the Miaojiaba dam. (b) Typical section of the Miaojiaba dam

0 + 63, 0 + 135, 0 + 194 and 0 + 254. In total, eight monitoring lines (TC1–TC8) were placed in the four cross-sections, where three monitoring lines were placed in section 0 + 194 (Figure 4(a)). The longitudinal deformations of the abutments were measured using the five-coupled soil displacement gauges distributed along the axis section of the dam. Four monitoring lines were placed in the dam axis section: two monitoring lines (ID1 and ID2) in the left abutment at 791 and 796 m elevations and

Downloaded by [UNIV OF ILLINOIS] on [05/02/20]. Copyright © ICE Publishing, all rights reserved.

Parameters	Values	Parameters	Values
Maximum height	111 m	Downstream integrated dam slope	1:1·55
Crest elevation	805 m	Reservoir volume	$2{\cdot}68 \times 10^9$ m^3
Crest length	348·20 m	Installed capacity	240 MW
Crest width	10·0 m	Annual energy generation	$9{\cdot}24 \times 10^9$ kW h
Upstream dam slope	1:1·4	Operational water level	800 m

Table 1. Parameters of the Miaojiaba project

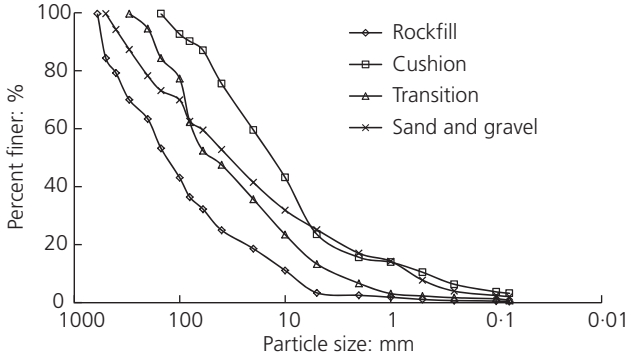

Figure 2. Gradation curve of different construction materials

two monitoring lines (ID3 and ID4) in the right abutment at the same elevations. The horizontal displacements of the dam body and foundation were measured using a vibrating wire displacement meter, including 22 monitoring points along four monitoring lines in cross-section 0 + 194, as shown in Figure 4(b). The behaviour of the cut-off wall was measured using a fixed inclinometer placed inside the wall. Figure 5(b) shows a part of the measuring points. The stresses inside the dam body were measured using a vibrating wire earth pressure cell distributed in cross-section 0 + 199. Stress change inside the dam causes deformation of the responsive plate of the earth pressure cell. The deformation is passed to the vibrating wire and transformed into vibrating wire stress changes, thereby changing the vibration frequency of the vibrating wire. The frequency signal is transmitted to the reading device through a cable. The stress inside the dam could then be obtained based on a preset algorithm. In total, 32 monitoring gauges along four monitoring lines were placed in the section, as shown in Figure 4(b).

4. Numerical model

4.1 Constitutive models and interface analysis method

The reliability of the numerical results depends significantly on the suitability of the constitutive model for the dam materials and proper modelling of the rockfill-slab and cut-off wall–foundation interaction. Thus far, various models have been proposed to model rockfills, such as the Lade model (Lollino *et al.*, 2005), elasto-plastic model (Zhang and Zhang, 2009), creep model (Zhou *et al.*, 2011) and generalised plasticity model (Xu *et al.*, 2012). Among these models, the non-linear elastic Duncan–Chang E-B model is the most widely used method in CFRD construction simulation (Zhang *et al.*, 2004). The E-B model is considered highly suitable for describing the behaviour of rockfill and sand and gravel materials compared with the in situ measurement results of CFRDs in service.

In this paper, instantaneous deformation (i.e. no time-dependent

Zone	Materials description	Maximum particle size: mm	Construction techniques	
			Layer thickness: m	Compaction
Rockfill	Quarry rock, metamorphic tuff	800	0·85	25 t towed vibratory roller, ten passes
Cushion	Blended sand and gravel	150	0·45	20 t self-propelled vibratory roller, eight passes
Transition	Selected rock, processed metamorphic tuff	300	0·45	20 t self-propelled vibratory roller, eight passes
Sand and gravel	Sand and gravel, gravel	600	44–50	25 t towed vibratory roller, ten passes

Table 2. Construction materials and methods details for Miaojiaba CFRD

Downloaded by [UNIV OF ILLINOIS] on [05/02/20]. Copyright © ICE Publishing, all rights reserved.

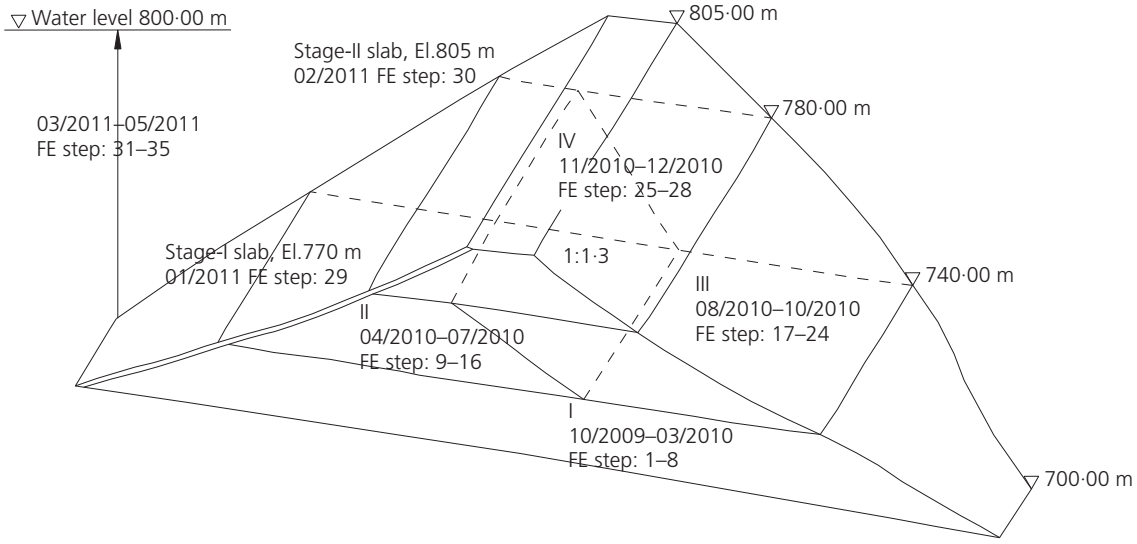

Figure 3. Construction scheme of the Miaojiaba dam

soil behaviour) of the rockfill and sand and gravel materials was described using the E-B model. Triaxial tests were carried out using the construction materials of Miaojiaba CFRD. The tested rockfill materials had the same rock origin, but smaller particles were obtained using the parallel gradation technique (Xu *et al.*, 2012) for triaxial testing and had a maximum particle size of 80 mm. The computational parameters for the E-B model deduced from the triaxial tests results are listed in Table 3. The concrete slab, toe slab and cut-off wall materials were simulated using a linear elastic model. The density and Poisson ratio of the concrete material are 2·45 g/cm^3 and 0·167, respectively. The elastic moduli for the slab and toe slab were both 28 GPa, while that for the cut-off wall was 26 GPa. The face slab and cut-off wall strongly interacted with the adjacent gravel layer because of the significant difference in their stiffness. In this paper, interaction was modelled using the no-thickness friction contact method based on the Adina system (Bathe, 2003).

4.2 Finite-element modelling

The structure module of Adina 8.5 software (Adina R&D, Inc.) was used to model the behaviour of the Miaojiaba CFRD. The finite-element (FE) mesh of the dam used for the static calculation is presented in Figure 5. The FE mesh has a total of 67 185 elements and 73 184 nodes. The different parts of the model were simulated using the spatial eight-node isoparametric elements. The sand and gravel foundation is divided into three layers based on geological characteristics. The construction process and subsequent reservoir filling were simulated as realistically as possible in the numerical procedure. The simulation of the construction process is illustrated in Figure 3. Since time is not taken into account in the analysis, the dates shown in the model and results refer to the real construction sequence. The simulated thickness of each layer was less than 5 m. To simulate the entire section construction scheme, FE steps 17–24 were merged with steps 9–16. The bottom boundary of the FE model was fixed along the x, y and z directions. The side boundaries of the model were constrained in the normal direction. The reservoir pressure of upstream was simulated as a surface force on the slabs. The FE analysis was conducted to analyse and evaluate the behaviour of the dam and improve its design and construction, which was carried out before dam construction commenced.

5. Results and discussion

5.1 Stress–deformation behaviour of the CFRD built on the sand and gravel foundation

The behaviour of the dam body and its seepage control system were analysed by correlating the field measurements and the results of the numerical simulation. The field measured data were utilised to assess the behaviour of the CFRD and validate the numerical model adopted in this study. Figure 6 shows the plot of measured and simulated cumulative settlement distribution in cross-sections 0 + 192 and 0 + 194 after construction. The following inferences could be realised from these cross sections. (*a*) Maximum settlement occurred near the base of the dam at an elevation of approximately 720 m instead of the mid-height, because of the presence of the sand and gravel foundation. The maximum cumulative settlements of the foundation and dam body are 0·47 and 0·72 m, respectively. (*b*) The field measured results of the settlements are slightly higher than the numerical simulation in the central region, but slightly smaller in the external region. The maximum difference in the magnitude is approximately 0·18 m, which may have arisen from numerical model and measurement errors. (*c*) The FE results showed a trend similar to that of the field measurement results, with the magnitude of the settlement being consistent in both methods.

The measured and simulated deformation of several monitoring

Downloaded by [UNIV OF ILLINOIS] on [05/02/20]. Copyright © ICE Publishing, all rights reserved.

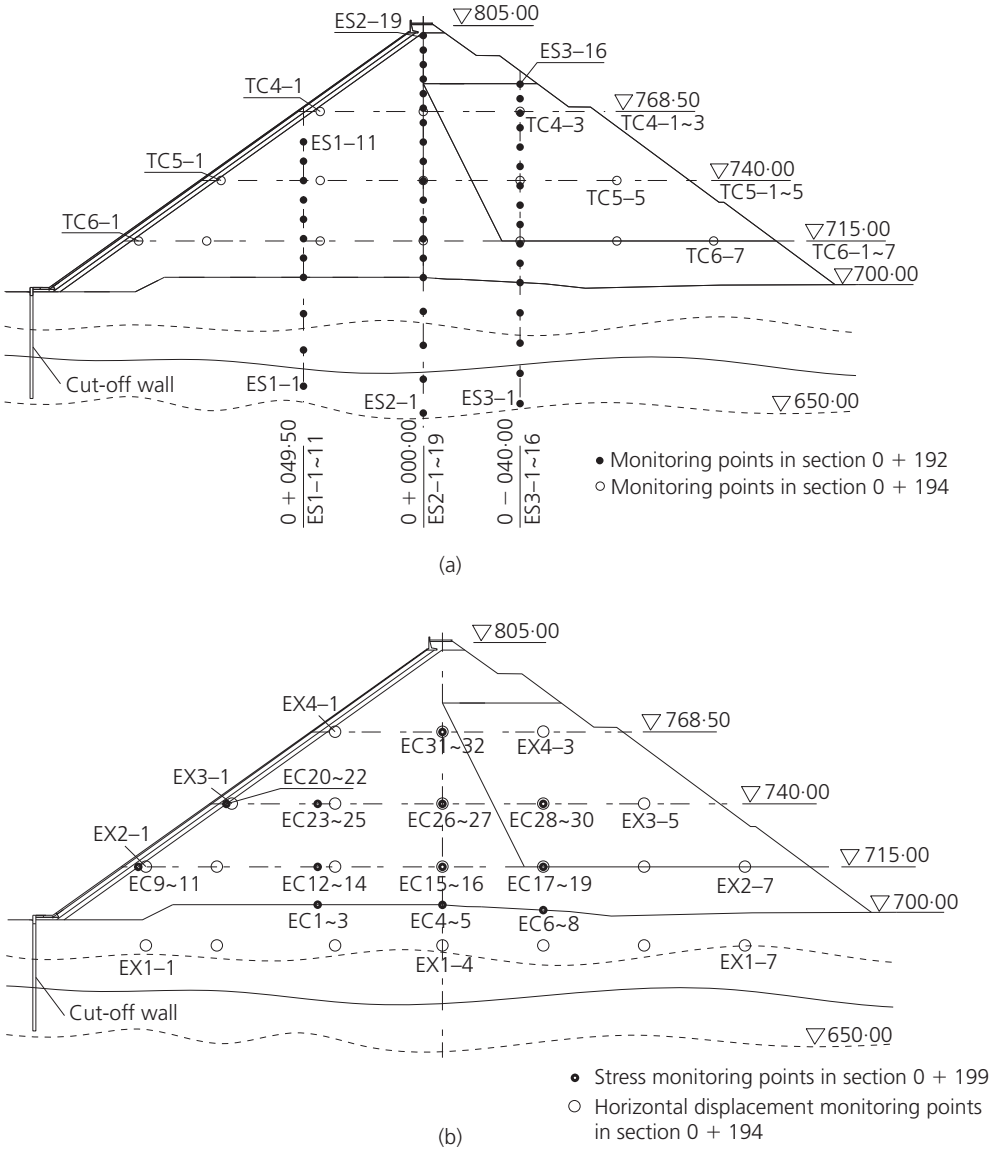

Figure 4. Layout of the monitoring system: (a) settlement monitoring points in the cross-sections 0 + 192 and 0 + 194; (b) stress and displacement monitoring points in the cross-section 0 + 199 and 0 + 194

points were determined and plotted in Figure 7. The results indicated the cumulative vertical and horizontal displacements over dam construction. The continuous raising of the dam during construction rapidly increased deformation. Increase in deformation lessened during the later construction phase, where the settlement rate inside the dam body was less than 1 mm per month. The settlements of the dam gradually stabilised after the later construction phase; however, impoundment caused a certain incremental deformation. The dam settlement is mainly caused by compressive deformation of the rockfill, which is a kind of dispersing material with hard, solid particles. The compressive deformation is mainly caused by structure adjustment of the skeleton particles and particle breakage. During construction, intense structure adjustment and a small amount of particle breakage occur in the rockfills and foundation under the effect of dam weight and dam compaction, which cause most of the cumulative settlement of the dam. As shown in Figure 7, most of the settlement (more than 80% of the total settlement) occurs during the construction period. The constitutive model that is used, such as the present model, does not take into consideration the factor of creep deformation. Therefore, the simulated results of the maximum settlement (Figure 7(b)) and the longitudinal displacement (Figure 7(d)) are lower than the field measurements during the construction. However, the simulated deformation magnitudes and the trend are

Downloaded by [UNIV OF ILLINOIS] on [05/02/20]. Copyright © ICE Publishing, all rights reserved.

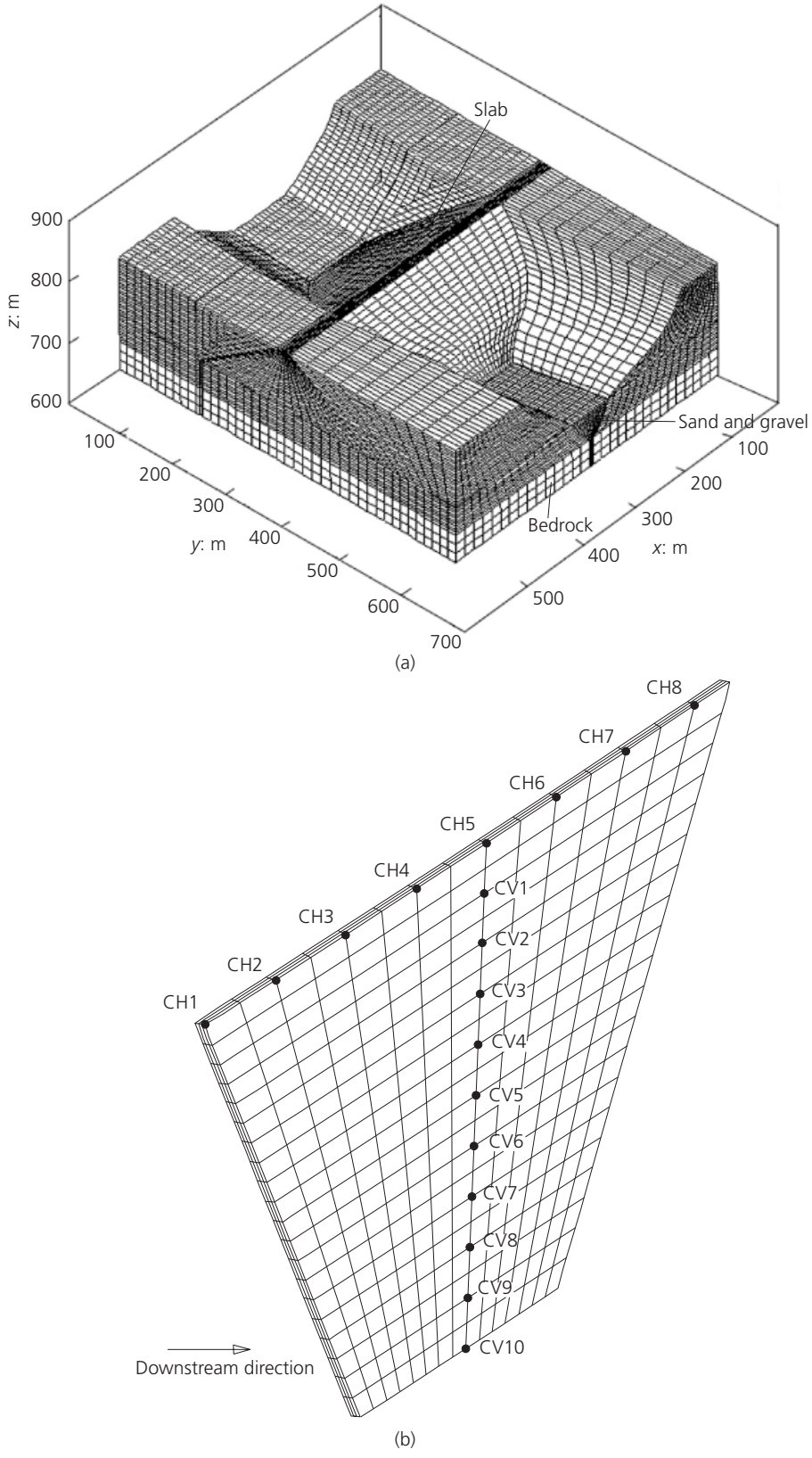

Figure 5. Three-dimensional FE mesh of the Miaojiaba dam: (a) mesh of the dam; (b) mesh of the cut-off wall

Downloaded by [UNIV OF ILLINOIS] on [05/02/20]. Copyright © ICE Publishing, all rights reserved.

Material	Density: g/cm^3	K	n	K_{ur}	ϕ_0: degrees	n_{ur}	C: kPa	R_f	K_b	m
Cushion zone	2·25	1400	0·42	2200	49	0·38	0	0·85	750	0·20
Transition zone	2·23	1300	0·42	2100	49	0·38	0	0·85	740	0·20
Main rockfill zone	2·30	1250	0·45	1950	53	0·40	0	0·90	600	0·40
Sub rockfill zone	2·15	1050	0·35	1450	52	0·39	0	0·81	570	0·32
Sand and gravel ($Q_4^{al} - 1$)	2·05	1000	0·43	1500	43	0·43	0	0·78	550	0·30
Sand and gravel ($Q_4^{al} - 2$)	2·05	1200	0·43	1700	42	0·43	0	0·80	600	0·30
Sand and gravel ($Q_4^{al} - 3$)	2·10	1500	0·42	2000	41	0·42	0	0·81	650	0·20

K, modulus number; n, modulus exponent; K_{ur}, unloading modulus number; ϕ_0, friction angle; n_{ur}, unloading modulus exponent; C, cohesion intercept; R_f, failure ratio; K_b, bulk modulus number; m, bulk modulus exponent.

Table 3. Computational parameters of the E-B model

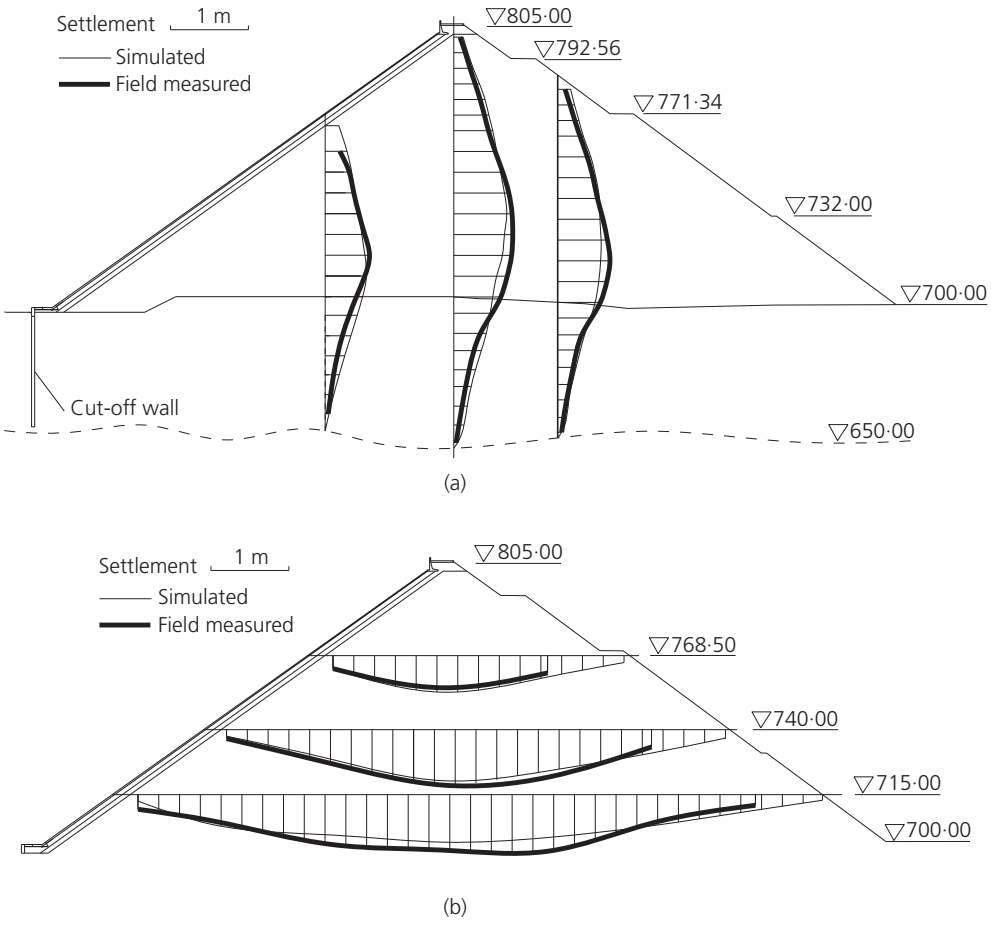

Figure 6. Measured and simulated settlement of the dam in: (a) section 0 + 192; (b) section 0 + 194

in good agreement with the field measurements. Tables 4 and 5 list and compare the stresses and deformations at several typical monitoring points after construction. Overall, the simulated and measured stresses and deformations are almost consistent, which suggests that the numerical procedure could accurately describe the behaviour of the Miaojiaba CFRD.

Reservoir filling is a critical loading condition for dams, in which

Downloaded by [UNIV OF ILLINOIS] on [05/02/20]. Copyright © ICE Publishing, all rights reserved.

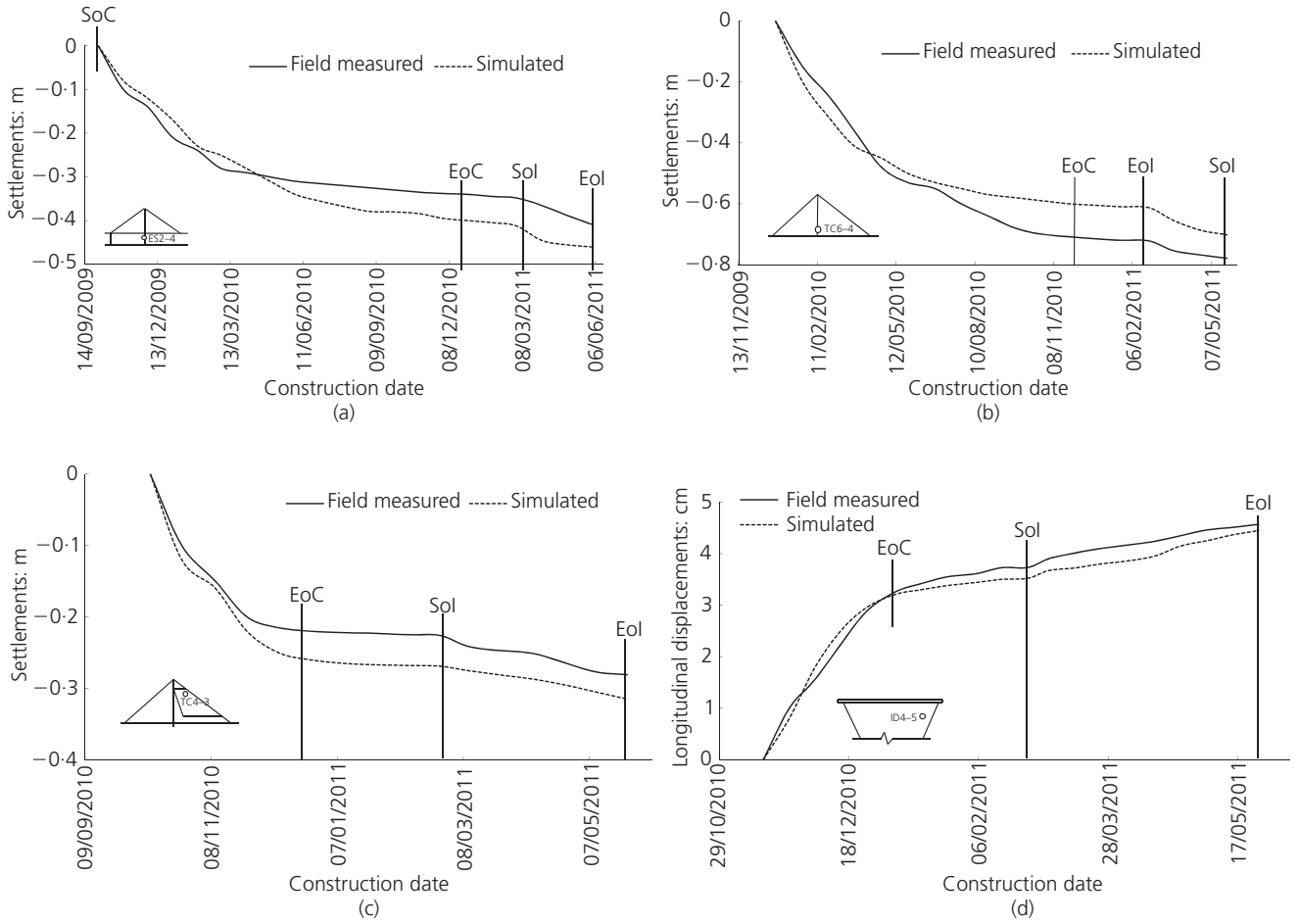

Figure 7. Comparison of the simulated deformation history and field measurements taken at monitoring points (SoC, start of construction; EoC, end of construction; SoI, start of impounding; EoI, end of impounding): (a) monitoring point ES2-4; (b) monitoring point TC6-4; (c) monitoring point TC4-3; (d) monitoring point ID4-5

Measuring points	Stress *z*: kPa (measured)	Stress *z*: kPa (simulated)	Measuring points	Stress *y*: kPa (measured)	Stress *y*: kPa (simulated)
EC4	1752	1785	EC5	192	270
EC6	1680	1625	EC7	202	245
EC12	869	670	EC13	118	185
EC20	35	60	EC21	161	210
EC28	420	670	EC29	5	35
EC31	125	320	EC32	68	110

Note: compressive stress is positive.

Table 4. Stresses at the typical monitoring points of the cross-section 0 + 199 after construction

the reservoir pressure causes horizontal and vertical displacements. Figure 8 shows incremental deformations in the dam caused by reservoir filling. The results showed that the reservoir pressure causes significant incremental deformation, especially for horizontal displacement. The maximum incremental settlements caused by the reservoir pressure occurred close to the bottom of the upstream face slab and diminished towards the downstream face. The reservoir pressure pushed the dam

Downloaded by [UNIV OF ILLINOIS] on [05/02/20]. Copyright © ICE Publishing, all rights reserved.

Measuring points	Settlement: m		Measuring points	Horizontal displacement: mm		Measuring points	Longitudinal displacement: cm	
	Measured	Simulated		Measured	Simulated		Measured	Simulated
ES1-3	0·22	0·33	EX1-1	−85·6	−99·5	ID1-1	−1·56	−1·39
ES1-6	0·57	0·51	EX2-2	−70·2	−68·1	ID1-5	−2·61	−2·54
ES1-9	0·37	0·38	EX3-2	−22·1	−28·2	ID2-1	−1·02	−1·51
ES2-4	0·34	0·42	EX4-1	−8·5	−7·6	ID2-5	−3·89	−3·71
ES2-7	0·71	0·62	EX1-7	79·6	87·2	ID3-1	0·97	0·91
ES3-4	0·31	0·35	EX2-7	45·3	53·4	ID3-5	2·57	2·31
ES3-7	0·67	0·56	EX3-5	19·7	25·6	ID4-1	1·12	1·02
ES3-10	0·51	0·53	EX4-3	8·6	10·7	ID4-5	3·73	3·50

Note: The positive direction of the horizontal displacement points to downstream and the positive direction of the longitudinal displacement points to the left bank.

Table 5. Cumulative deformations at typical monitoring points after construction

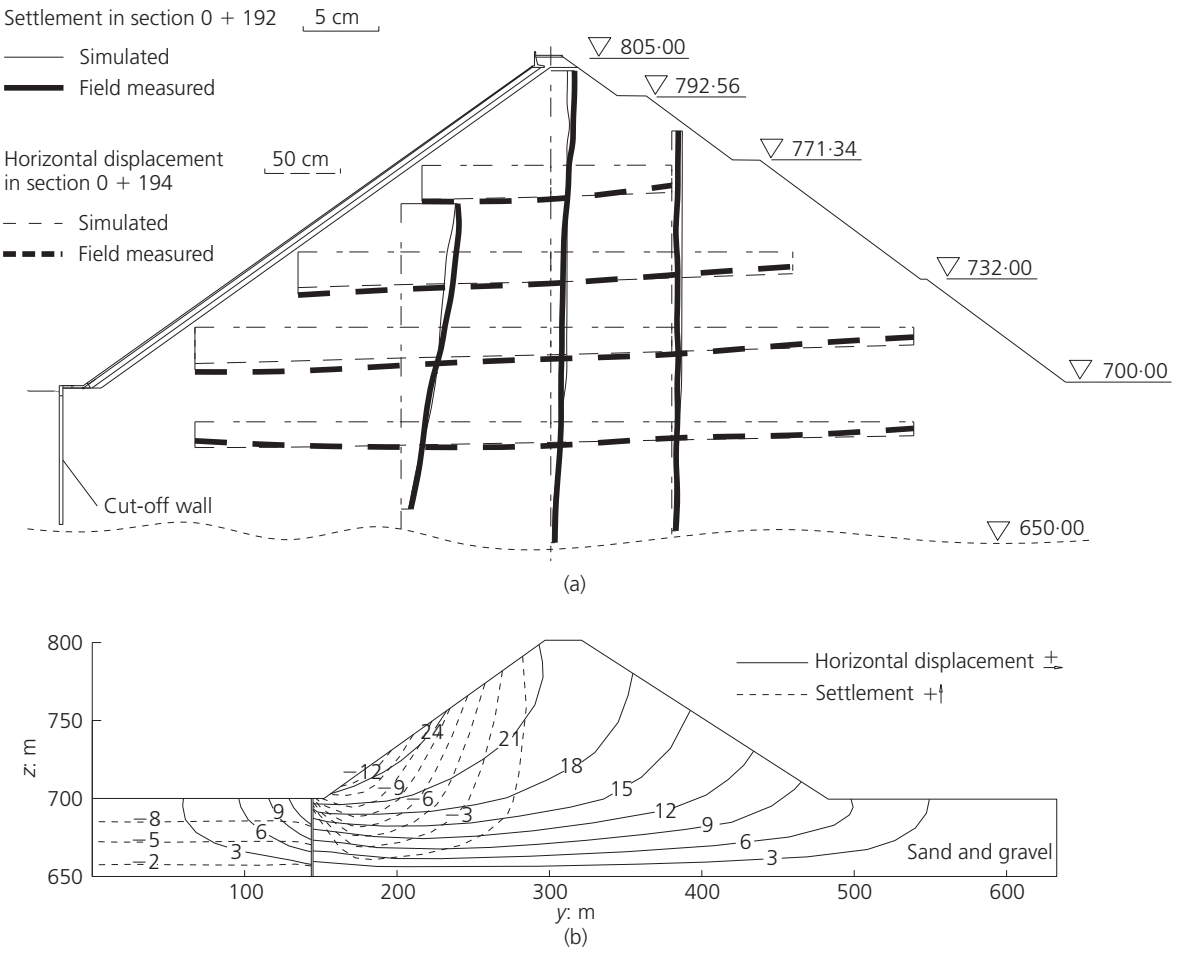

Figure 8. Incremental deformations caused by the reservoir filling: (a) field measured and simulated incremental deformations; (b) simulated incremental deformation distribution in the cross-section 0 + 192 (unit: cm)

Downloaded by [UNIV OF ILLINOIS] on [05/02/20]. Copyright © ICE Publishing, all rights reserved.

downstream, thereby causing maximum horizontal displacement of about 25 cm close to the upstream face slab. During construction, the deformation trend of the dam is symmetrical at approximately the centre-line of the dam. However, the incremental deformations caused by reservoir pressure showed a significantly different pattern of movements from the construction movements.

Figure 9 shows the cumulative settlement and vertical total stress contours of the cross-section 0 + 192 after reservoir filling. The maximum settlement of 0·83 m, which is about 0·75% of the dam height, occurred at the bottom of the dam body. The maximum cumulative settlement after reservoir filling is larger than the settlement after construction, which could obviously be attributed to the water load. The maximum compressive stress in the foundation is about 2·5 MPa. A significant arching effect is shown. The distribution of the minor principal stress is similar to that of the compressive stress. The measured and simulated results suggest that the Miaojiaba CFRD is well constructed.

Time is not taken into account in the analysis. Creep of the rockfill and consolidation of the foundation due to pore-water pressure dissipation during dam construction could influence the dam behaviour if time-dependent soil behaviour was taken into account. The time-dependent soil behaviour would cause larger deformation of the dam body and result in some increase of the stress and deformation of the impervious structures during dam construction and reservoir filling. However, the time-dependent behaviour is mainly responsible for the long-term dam performance and its influence on the dam behaviour during dam construction and reservoir filling is limited. The numerical model in the paper could model the dam behaviour with reasonable accuracy.

5.2 Effect of the staged construction scheme on the dam behaviour

As shown in Figure 3, the dam body is not constructed by the entire section construction scheme, which is the alternative scenario for the construction of the Miaojiaba CFRD. In this study, the behaviour of the dam constructed by the entire section was simulated to analyse the difference. The FE steps were described previously, and the reservoir filling process was simulated as explained in the previous scheme.

The upstream and downstream sections of the dam body have different deformation timings under staged construction scheme. The upstream section was constructed and deformed to stable before the construction of the downstream section. The larger deformation of the new constructed downstream section caused

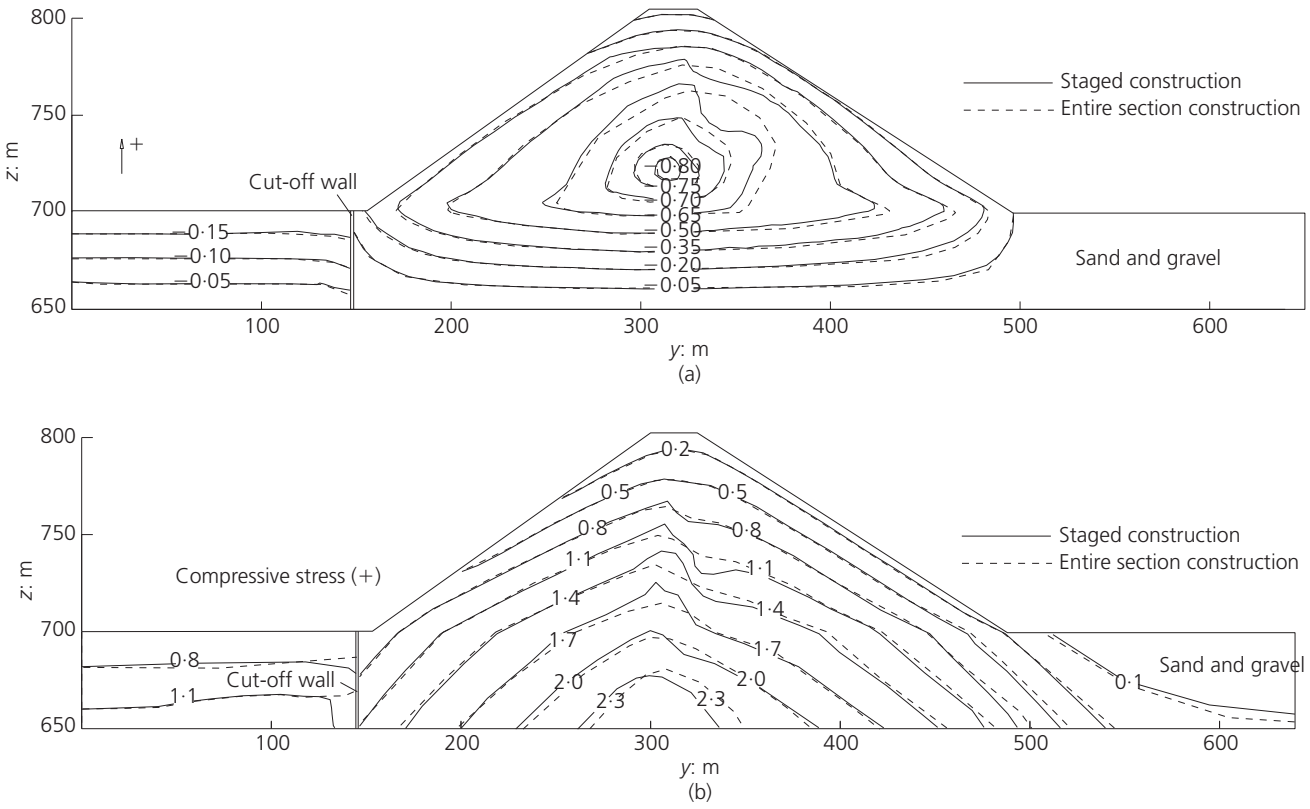

Figure 9. Cumulative settlement and vertical total stress contours of the cross-section 0 + 192 after reservoir filling: (a) cumulative settlement (unit: m); (b) vertical total stress (MPa)

Downloaded by [UNIV OF ILLINOIS] on [05/02/20]. Copyright © ICE Publishing, all rights reserved.

significant differential settlement difference between the upstream and downstream sections. Given that the upstream section of the dam body has deformed to stable, the downstream section causes little incremental deformation in these parts. Based on the above analysis, deformation of the dam body and foundation is mainly determined by the weight of the upstream section rockfill body under staged construction scheme during construction, whereas deformation is mainly determined by the weight of the entire section under the entire section scheme. Therefore, staged construction scheme of the dam will cause smaller horizontal displacement and settlement, but uneven deformation and stress concentration, especially when the dam is built on a sand and gravel foundation. Figure 9 shows a comparison of the deformation and stress results. The settlements and longitudinal displacement under the entire section scheme are larger than those in the actual construction scheme, as explained above. However, the deformation and stress results showed a similar trend. The observed differences in the settlement and stress mainly occurred in the parts that connect the upstream and downstream sections. The entire section scheme could improve the stress state and inhomogeneous deformation of the dam body to some extent, but causes larger deformation during construction.

5.3 Behaviour for the impervious structures

Reliability of the seepage control system is the most critical issue for a CFRD built on sand and gravel foundation. During construction, the dam construction and settlements cause horizontal separation between the connecting plate and the cut-off wall, as well as between the connecting plate and the toe slab. However, the differential settlement between the connecting plate and the cut-off wall is insignificant. Upon reservoir filling, the connecting plate and the face slab generate large settlement under the effect of water load and foundation settlement, further increasing the differential settlement between the connecting plate and the cut-off wall, as well as the horizontal separation distance between the connecting plate and cut-off wall. The maximum separation distance and differential settlement were 6 and 5 cm, respectively, whereas those between the connecting plate and the toe slab were 3·5 and 2·9 cm, respectively.

The longitudinal deformation of the dam body is larger than the face slab after reservoir filling, which causes great shear stress on the slab. The shear stress causes compressive stress at the centre part of the slab and tensile stress at both sides of the bottom. Similarly, the differential settlement between the dam body and the face slab causes compressive stress at the bottom of the slab and tensile stress at the top. Under the effect of the reservoir pressure and foundation deformation, maximum deflection of 14·88 cm occurred in the central region and near the bottom of the slab. The significant deflection also caused some tensile stress in the peripheral part. The maximum simulated compressive stress was 6·73 MPa and the maximum tensile stress was 1·61 MPa at both sides of the bottom. The toe slab and the connecting plate are mainly exposed to compressive stress under loading of the reservoir pressure and soil compressive stress. Given the constraints of the rock, a small-scale region at both sides of the connecting plate is exposed to the tensile stress with a maximum value of 0·71 MPa. These results suggest that the sand and gravel foundation has a significant effect on the behaviour of the seepage control system.

5.3.1 Behaviour of the cut-off wall

Thus far, many studies have examined the behaviour of the face slab, but few have examined the cut-off wall. In this study, the focus is on the behaviour of the cut-off wall and its influencing factors. Typically, the cut-off wall in the foundation endures complex loading. Both sides of the wall undergo soil compressive stress from foundation, and the magnitude is larger at the centre part of the wall because of the larger horizontal displacement of the adjacent soil. The simulated maximum soil compressive stress is 13·51 MPa at the downstream face during construction and 28·21 MPa at the upstream face after reservoir filling. Given the differential settlements between the wall and the foundation, the wall undergoes significant shear stress from the foundation. During construction, the downstream soils of the wall are compressed, but the upstream soils are uplifted. The wall undergoes downward shear stress in the downstream face and upward shear stress in the upstream face. The simulated maximum downward shear stress is 2·03 MPa at the centre of the downstream face. Upon subsequent reservoir filling, both soils were compressed, and the wall mainly underwent downward shear stress with the maximum of 4·23 MPa at the upstream face. The shear stresses are associated with the relative displacement between the wall and soils. The soil compressive stress and shear stress caused significant compressive stress in the wall. Reaction forces from the rock were mainly distributed at both sides of the wall. The complex force state induced the complex behaviour of the wall.

Figure 10 shows the measured and simulated results of the upstream displacement at the monitoring points after construction. The FE results under the actual construction scheme (staged construction) are smaller than the field measurement results, which may be due to the numerical model and measurement errors. However, they show a similar trend. During construction, the wall deformed upstream under the effect of larger horizontal displacement of the downstream foundation. The maximum measured upstream displacement of about 7 cm occurred at the top and near the centre of the wall. Figure 11 shows the simulated incremental deformations and stresses caused by the reservoir filling. Upon reservoir filling, the reservoir pressure pushes the wall downstream with a simulated maximum displacement increment of about 15 cm at the top of the wall and measured increment of about 13 cm. Given that the bottom and sides of the wall are constrained by the bedrock, the sides and bottom of the upstream face of the wall undergo greater positive bending moments under the effect of wall deflection and bedrock constraints. The bending moments cause tensile stress at the sides and bottom of the upstream face of the wall, as shown in Figure 11, and further cause tensile stress at the upstream face after

Downloaded by [UNIV OF ILLINOIS] on [05/02/20]. Copyright © ICE Publishing, all rights reserved.

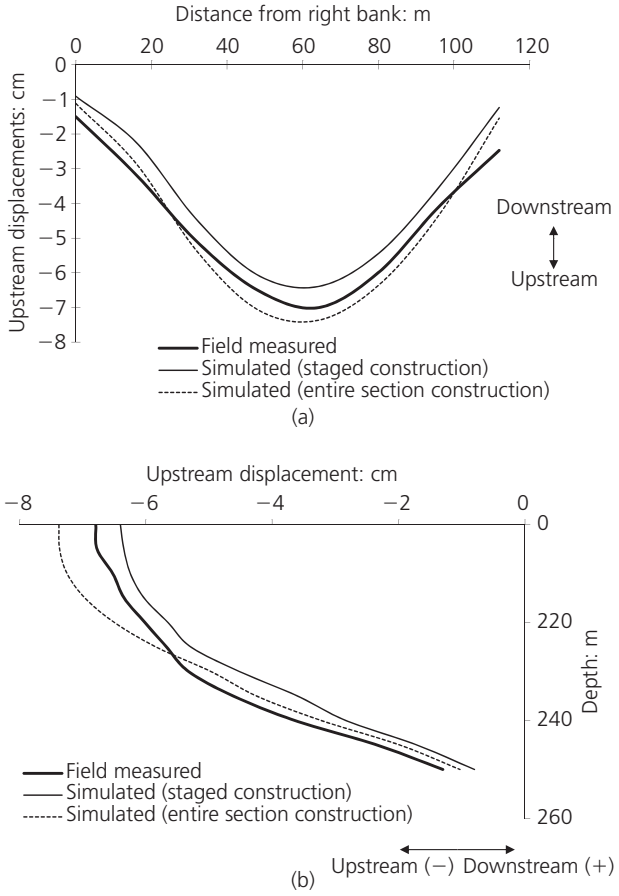

Figure 10. Upstream displacement of the cut-off wall after construction in: (a) wall crest; (b) wall axis

reservoir filling. The shear stress caused by differential longitudinal deformation between the wall and foundation also causes certain tensile stresses in the wall.

Figure 12 displays the simulated stress distribution in the cut-off wall after reservoir filling. The wall mainly displays tensile stress in the upstream face and compressive stress in the downstream face, as explained previously. The maximum compressive stress of 14·8 MPa occurred in the downstream face, and the maximum tensile stress of 4·25 MPa was observed in both sides of the upstream face. The stress state of the wall during construction was also computed. The wall deformed upstream under the downstream soil thrust. The wall bent upstream because of the constraints of the bedrock, thereby causing tensile stress at the bottom of the downstream face. The maximum tensile stress and compressive stress are smaller than the corresponding values of 1·92 and 6·49 MPa, respectively, after reservoir filling. The calculated tensile stress of the cut-off wall is relatively larger in this paper because of the numerical model, calculation parameters and boundary conditions. In general, the cut-off wall is mainly exposed to the compressive stress.

5.3.2 Effect of the dam construction scheme

Figures 10 and 12 show the stress and deformation results of the cut-off wall under the entire section scheme with a trend similar to those in the actual construction scheme. As previously analysed, horizontal displacement is mainly determined by the upstream section of the dam body under the staged construction scheme, but is determined by the entire section under the entire section scheme during construction. Thus, compared with the results under the staged construction scheme, the cut-off wall generates larger deformation during construction under the entire

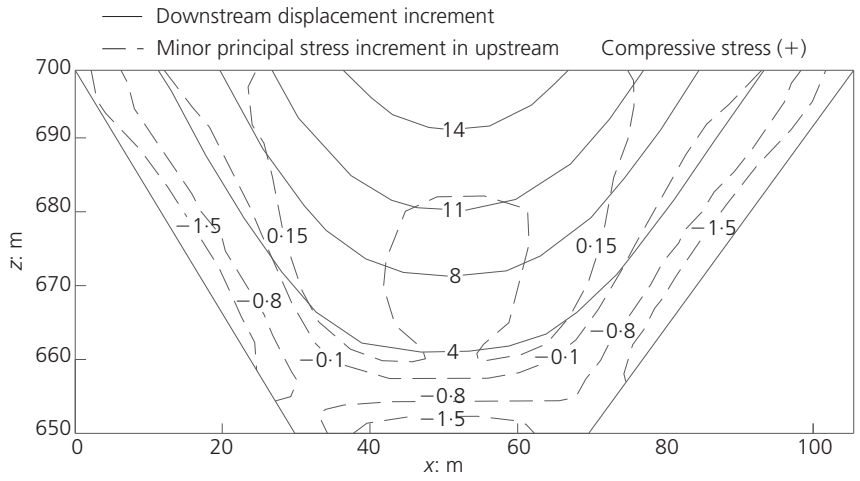

Figure 11. Downstream incremental displacement (unit: cm) and minor principal stress (unit: MPa) in upstream of the cut-off wall caused by the reservoir filling

Downloaded by [UNIV OF ILLINOIS] on [05/02/20]. Copyright © ICE Publishing, all rights reserved.

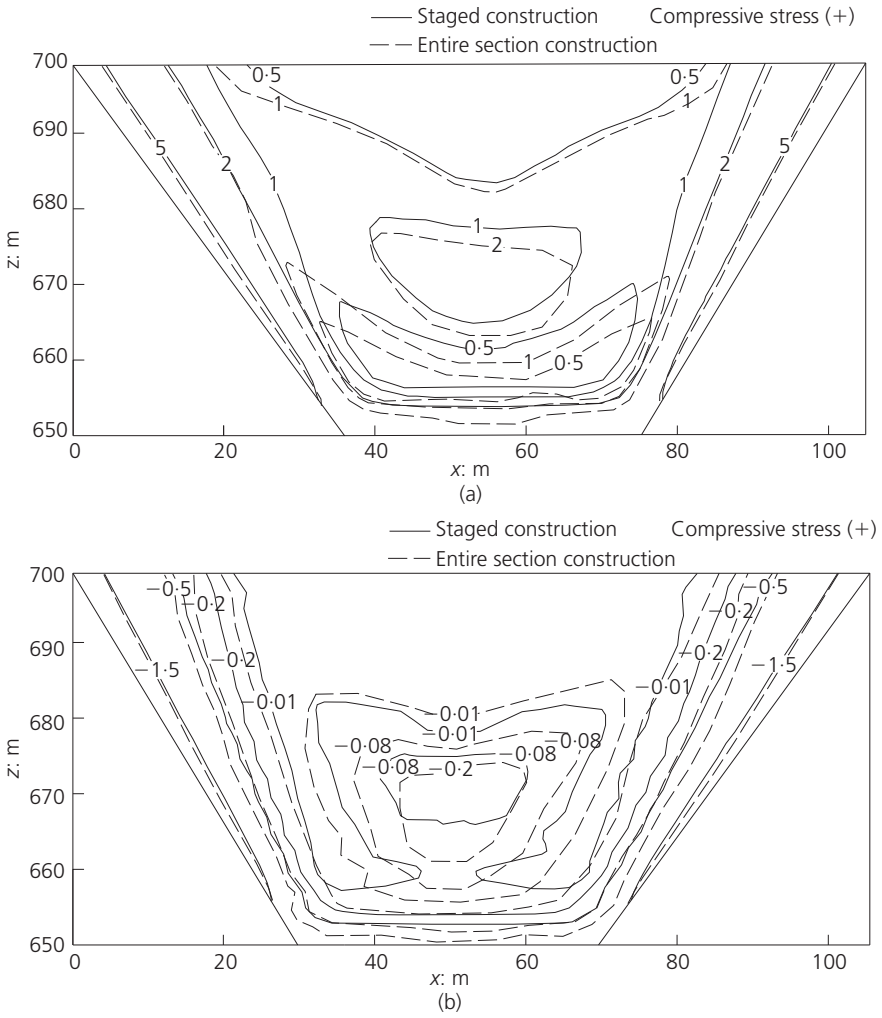

Figure 12. Stress distribution in the cut-off wall after reservoir filling (unit: MPa): (a) major principal stress in the downstream; (b) minor principal stress in the upstream

section scheme. The wall under the entire section scheme generates smaller downstream displacement after reservoir filling under the same water load because of larger upstream deformation. The wall undergoes larger compressive and tensile stress because of the shear stress caused by the larger differential in vertical and longitudinal deformation. This result implies that the staged construction scheme could reduce the stress of the wall to some extent after reservoir filling.

5.3.3 Effect of the construction sequence

The behaviour of the cut-off wall is directly related to its construction sequence. To gain deeper insights into this behaviour, the effect of the construction sequence was analysed in this study, taking into account the following two cases. Case A models the actual construction sequence of the wall, wherein the construction of the wall begins before the construction of the dam and is completed when the dam is constructed to an elevation of 710 m. In case B, the construction of the wall is started after the dam has been constructed to an elevation of 740 m.

When the wall is constructed under case B, the incremental horizontal displacement of the foundation and the differential settlement between the wall and the foundation are reduced significantly because the foundation generated a certain deformation before the construction of the wall. Therefore, the wall undergoes smaller shear stress and soil compressive stress. The smaller loadings cause significantly smaller deformation and stress. Figure 13 presents a comparison of the deformation predicted in both cases A and B. Smaller deformations are generated both during the completion and the operation periods when the cut-off wall was constructed under case B. Figure 14 shows a comparison of the stress level (ratio of actual principal stress difference and the principal stress difference at failure of the material) of the cut-off wall after reservoir filling. The stress

Downloaded by [UNIV OF ILLINOIS] on [05/02/20]. Copyright © ICE Publishing, all rights reserved.

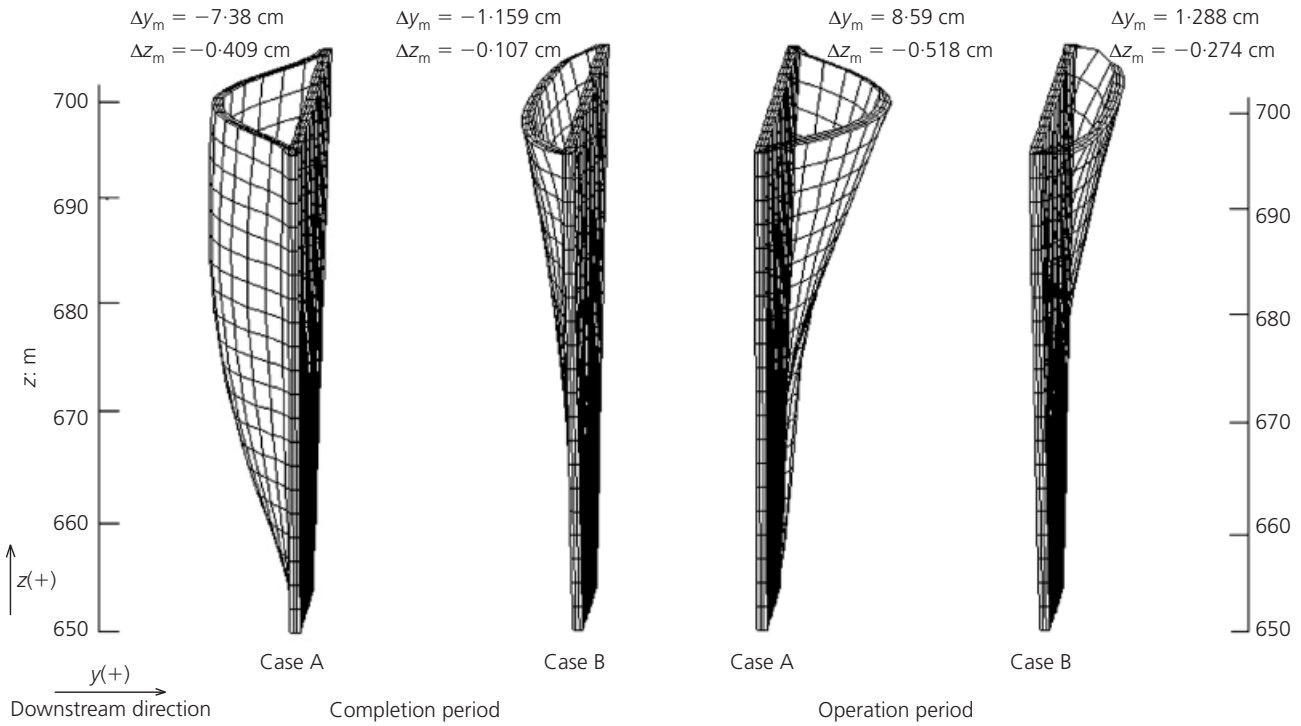

Figure 13. Deformations of the cut-off walls under two different construction schemes

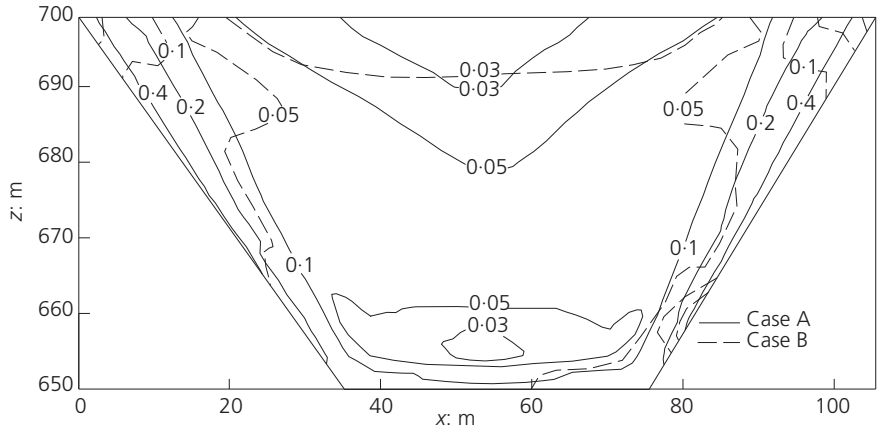

Figure 14. Stress level in the downstream face of the cut-off wall after reservoir filling under two different construction schemes

level is smaller than 1 in both cases. Given the significant reduction of the loading, the stress state of the wall was greatly improved.

5.3.4 Effect of depth

Currently, suspended cut-off walls are widely used in CFRDs. The required cut-off wall depth mainly depends on the dam height and the river gravel depth. The depths of the wall are assumed to be 50 (cutting off the sand and gravel), 45, 40, 35, 30 and 25 m to investigate the effect of depth on the behaviour. The wall was simulated by the actual construction sequence. The results of the cumulative upstream/downstream displacement and major principal stress in the axis of the cut-off wall with different depths are presented in Figure 15.

The bottom of the suspended wall is not constrained by the

Downloaded by [UNIV OF ILLINOIS] on [05/02/20]. Copyright © ICE Publishing, all rights reserved.

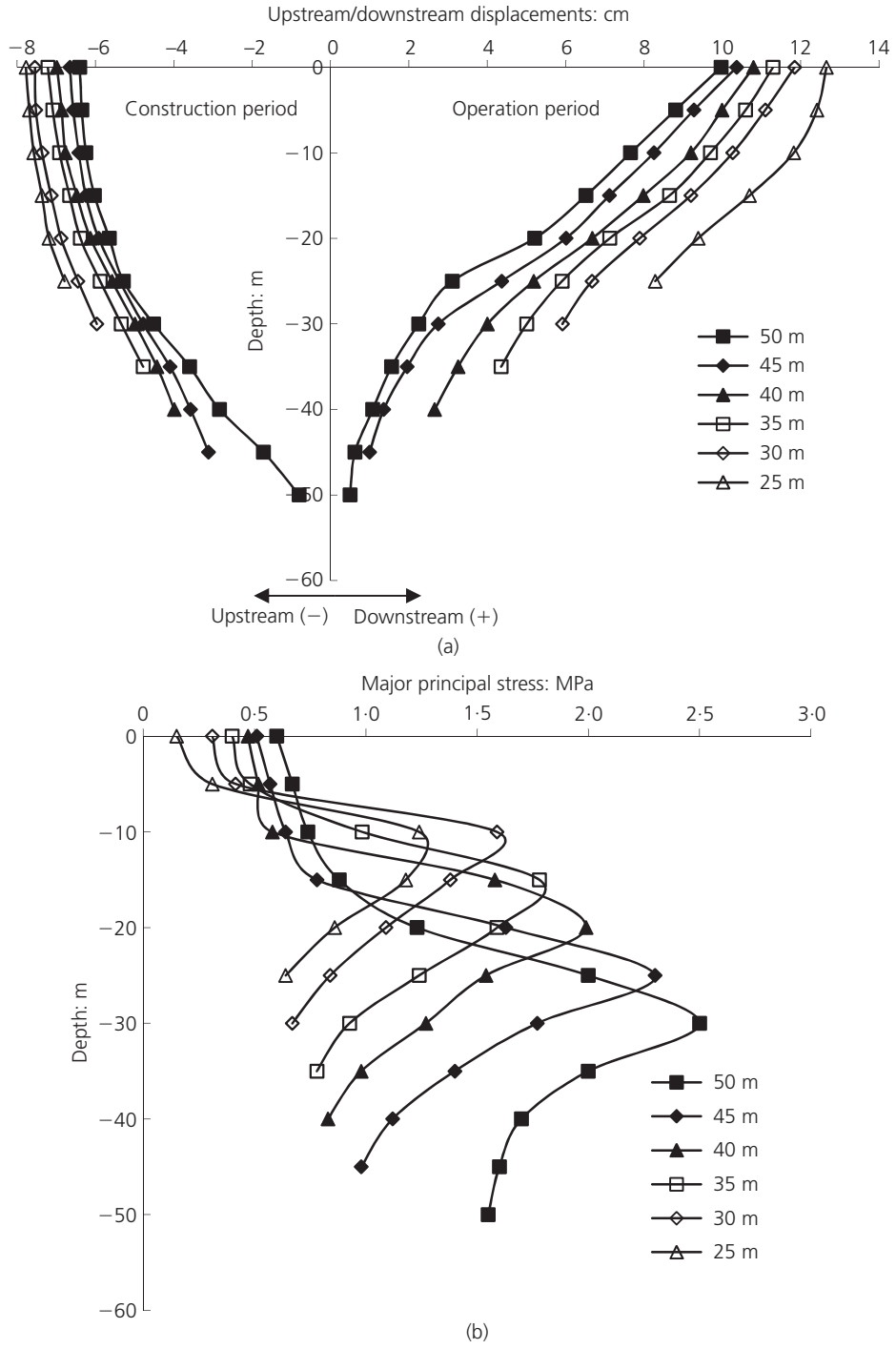

Figure 15. Cumulative deformation and stress at the axis of the cut-off wall with different depths: (a) upstream/downstream displacements; (b) major principal stresses in the downstream after reservoir filling

bedrock again, so the wall generated larger deformation and further reduced the differential settlement between the wall and the foundation. With the reduction of differential settlement, the soil shear stress decreased, which is the main loading that causes the stress in the cut-off wall. Compared with the results of the closed wall, the suspended cut-off wall generates larger deformation because of the change of the bedrock constraints. However, the walls exhibit a similar deformation trend. The downstream

Downloaded by [UNIV OF ILLINOIS] on [05/02/20]. Copyright © ICE Publishing, all rights reserved.

displacement of the 35 m wall increases by 13·3% during the operation period. The maximum compressive stress at the axis of the wall was observed at the centre, mainly under the effect of the soil shear stress. The compressive stress of the suspended wall tends to decrease because of the changes of constraints and decrease of the shear stress. Given that the bottom of the suspended wall is not constrained by the bedrock, the maximum tensile stress is distributed mainly on both sides under the effect of the deflection. These results suggest that a cut-off wall with a smaller penetration depth tends to be more safe and stable.

6. Conclusion

The behaviour of a CFRD built on sand and gravel foundation was analysed by monitoring the results and by performing numerical simulations. The simulated stress values and deformation trends and values at the monitoring points were consistent with the field measurements. The following inferences can be concluded.

(*a*) The sand and gravel foundation has a significant effect on the stress–deformation behaviour of the CFRDs. The results showed that the CFRD built on sand and gravel foundation could perform well.
(*b*) The entire section scheme can improve the stress state of the dam to some extent, but causes larger deformation during construction. When CFRDs are built with a staged construction scheme, the elevation difference between the upstream and downstream sections should be controlled at a small value.
(*c*) The cut-off wall in the sand and gravel foundation exhibits complex behaviour under the loads of soil compressive stress, shear stress and reservoir pressure. The entire section scheme may induce larger stress and deformation of the cut-off wall. However, a smaller penetration depth and construction of the wall when the constructed dam is raised at a larger height could improve the behaviour.

Acknowledgements

This study was supported by the programme 2013KCT-15 of the Shanxi provincial key innovative research team, special funds of the natural science foundation of Shanxi Province (2013JQ7010), China post-doctoral science foundation funded project (2014M562524XB and the national natural science foundation of China (51409206 and 51409208).

REFERENCES

Bathe KJ (2003) *Adina Theory and Modeling Guide, Volume I: Adina*. Adina R&D, Inc., Watertown, MA, USA, pp. 399–417.

Brown AJ and Bruggemann DA (2002) Arminou dam, Cyprus, and construction joints in diaphragm cut-off walls. *Géotechnique* **52(1)**: 3–13.

Chai J, Igaya Y, Hino T and Carter J (2013) Finite element simulation of an embankment on soft clay – Case study. *Computers and Geotechnics* **48**: 117–126.

Conti R, Sanctis L and Viggiani GMB (2012) Numerical modelling of installation effects for diaphragm walls in sand. *Acta Geotechnica* **7(3)**: 219–237.

Dounias GT, Anastasopoulos K and Kountouris A (2012) Long-term behaviour of embankment dams: seven Greek dams. *Proceedings of the Institution of Civil Engineers – Geotechnical Engineering* **165(3)**: 157–177, http://dx.doi.org/10.1680/geng.11.00052.

Feng DK, Zhang G and Zhang JM (2010) Three-dimensional seismic response analysis of a concrete-faced rockfill dam on overburden layers. *Frontiers of Architecture and Civil Engineering in China* **4(2)**: 258–266.

Gikas V and Sakellariou M (2008) Settlement analysis of the Mornos earth dam (Greece): evidence from numerical modeling and geodetic monitoring. *Engineering Structures* **30(11)**: 3074–3081.

Haan EJD and Feddema A (2012) Deformation and strength of embankments on soft Dutch soil. *Proceedings of the Institution of Civil Engineers – Geotechnical Engineering* **166(3)**: 239–252, http://dx.doi.org/10.1680/geng.9.00086.

Hinchberger S, Weck J and Newson T (2010) Mechanical and hydraulic characterization of plastic concrete for seepage cut-off walls. *Canadian Geotechnical Journal* **47(4)**: 461–471.

Ito M and Azam S (2013) Engineering properties of a vertisolic expansive soil deposit. *Engineering Geology* **152(1)**: 10–16.

Karim MR, Gnanendran CT, Lo SCR and Mak J (2010) Predicting the long-term performance of a wide embankment on soft soil using an elastic–viscoplastic model. *Canadian Geotechnical Journal* **47(2)**: 244–257.

Kim YS and Kim BT (2008) Prediction of relative crest settlement of concrete-faced rockfill dams analyzed using an artificial neural network model. *Computers and Geotechnics* **35(3)**: 313–322.

Li K, Ju Y, Han J and Zhou C (2008) Early-age stress analysis of a concrete diaphragm wall through tensile creep modeling. *Materials and Structures* **42(7)**: 923–935.

Lollino P, Cotecchia F, Zdravkovic L and Potts DM (2005) Numerical analysis and monitoring of Pappadai dam. *Canadian Geotechnical Journal* **42(6)**: 1631–1943.

Müller R, Larsson S and Westerberg B (2012) Stability for a high embankment founded on sulfide clay. *Proceedings of the Institution of Civil Engineers – Geotechnical Engineering* **166(1)**: 31–48, http://dx.doi.org/10.1680/geng.9.00080.

Özer AT and Bromwell LG (2012) Stability assessment of an earth dam on silt/clay tailings foundation: A case study. *Engineering Geology* **151**: 89–99.

Rice JD and Duncan JM (2010a) Deformation and cracking of seepage barriers in dam due to changes in the pore pressure regime. *Journal of Geotechnical and Geoenvironmental Engineering* **136(1)**: 16–25.

Rice JD and Duncan JM (2010b) Finding of case histories on the long-term performance of seepage barriers in dams. *Journal of Geotechnical and Geoenvironmental Engineering* **136(1)**: 2–15.

Segura CL and Aguado DCA (2012) Bi-layer diaphragm walls: evolution of concrete-to-concrete bond strength at early ages. *Construction and Building Materials* **31**: 29–37.

Su H, Hu J and Wen Z (2012) Structure analysis for concrete-

Downloaded by [UNIV OF ILLINOIS] on [05/02/20]. Copyright © ICE Publishing, all rights reserved.

faced rockfill dams based on information entropy theory and finite element method. *International Journal for Numerical and Analytical Methods in Geomechanics* **36(8)**: 1041–1055.

Szostak CA, Chrzanowski A and Massiéra M (2005) Use of deformation monitoring results in solving geomechanical problems – case studies. *Engineering Geology* **79(1–2)**: 3–12.

Wang YS and Liu SH (2005) Treatment for a fully weathered rock dam foundation. *Engineering Geology* **77(1–2)**: 115–126.

Won MS and Kim YS (2008) A case study on the post-construction deformation of concrete face rockfill dams. *Canadian Geotechnical Journal* **45(6)**: 845–852.

Xu B, Zou D and Liu H (2012) Three-dimensional simulation of the construction process of the Zipingpu concrete face rockfill dam based on a generalized plasticity model. *Computers and Geotechnics* **43**: 143–154.

Zhang B, Wang JG and Shi R (2004) Time-dependent deformation in high concrete-faced rockfill dam and separation between concrete face slab and cushion layer. *Computers and Geotechnics* **31(7)**: 559–573.

Zhang G and Zhang JM (2009) Numerical modeling of soil–structure interface of a concrete-faced rockfill dam. *Computers and Geotechnics* **36(5)**: 762–772.

Zhou W, Hua J, Chang X and Zhou C (2011) Settlement analysis of the Shuibuya concrete-face rockfill dam. *Computers and Geotechnics* **38(2)**: 269–280.

WHAT DO YOU THINK?

To discuss this paper, please email up to 500 words to the editor at journals@ice.org.uk. Your contribution will be forwarded to the author(s) for a reply and, if considered appropriate by the editorial panel, will be published as a discussion in a future issue of the journal.

Proceedings journals rely entirely on contributions sent in by civil engineering professionals, academics and students. Papers should be 2000–5000 words long (briefing papers should be 1000–2000 words long), with adequate illustrations and references. You can submit your paper online via www.icevirtuallibrary.com/content/journals, where you will also find detailed author guidelines.

Downloaded by [UNIV OF ILLINOIS] on [05/02/20]. Copyright © ICE Publishing, all rights reserved.